April 9, 2002

Mainz Microtron MAMI

Title: **Measurement of the Magnetic Dipole Moment of the $\Delta^+(1232)$ Resonance.**

Participants: J. Brudvik, B.M.K. Nefkens, S.N. Prakhov, J.W. Price, and A. Starostin, University of California, Los Angeles, CA, USA

J. Ahrens, J. Albert i Forte, H.J. Arends, R. Beck, D. Drechsel, D. Krambrich, M. Lang, S. Scherer, A. Thomas, L. Tiator, M. Vanderhaeghen, D. von Harrach and Th. Walcher, Institut für Kernphysik, Mainz, Germany

S. Altieri, A. Braghieri, A. Panzeri, P. Pedroni, and T. Pinelli, INFN, Sezione di Pavia and Department of Nuclear and Theoretical Physics, Pavia, Italy

J.R.M. Annand, J. Kellie, K. Livingston, J.C. MacGeorge, I.J.D. MacGregor, G. Rosner, and D.P. Watts, Department of Physics and Astronomy, Glasgow, UK

C. Bennhold and W. Briscoe, George Washington University, Washington, USA

S. Cherepnya, L. Fil'kov, and V. Kashevarow, Lebedev Physical Institute, Moscow, Russia

B. Krusche, Institut für Physik, Basel, Ch

M. Kotulla, J. Messchendorp, V. Metag, R. Novotny, M. Pfeiffer and S. Schadmand, II. Physikalisches Institut, Giessen, Germany

W. Meyer, Institut für Experimentalphysik, Bochum, Germany

V. Lisin, R. Kondratiev and A. Polonski, Institute for Nuclear Research, Moscow, Russia

H. Dutz, Physikalisches Institut, Bonn, Germany

D. Hornidge, Saskatchewan Accelerator Laboratory, Canada

P. Grabmayr and T. Hehl, Physikalisches Institut Universität Tübingen

J.R. Comfort, Arizona State University, Tempe, AZ

M. Manley, Kent State University, OH, USA

T.D.S. Stanislaus, Valparaiso University, Valparaiso, IN

Spokesmen: R. Beck, Inst. f. Kernphysik Becher-Weg 45 55099 Mainz Germany
Tel: 0049 6131 3922933, Fax: 0049 6131 3922964,
email: rbeck@kph.uni-mainz.de

M. Kotulla, II. Phys. Institut Universität Giessen
Tel: 0049 641 9933223, Fax: 0049 641 9933209,
email: Martin.J.Kotulla@exp2.physik.uni-giessen.de

A. Starostin, Dept. of Physics, UCLA
Tel: (310) 825-2259, Fax: (310) 206-4397,
email: starost@bmkn5.physics.ucla.edu

Time Request: 300 h engineering run; 600 h physics run

Abstract

We propose to determine the magnetic dipole moment of the $\Delta^+(1232)$ resonance from a measurement of the five-fold differential cross sections for the reaction $\gamma p \to \gamma' \pi^0 p$ in the region of the Δ resonance ($E_\gamma = 300-500$ MeV) and the photon asymmetry Σ for linearly polarized photons. We require a beam of tagged polarized photons incident on a liquid hydrogen target. The π^0, γ' and p final state particles are measured with the Crystal Ball large acceptance multiphoton spectrometer with the TAPS detector as forward wall detector. A central tracker detector will be used to measure the trajectory of the proton.

Contents

1 Introduction

The magnetic dipole moment, μ_b, of a baryon is due to the quark spins and to the average of the quark currents. As such the numerical value of μ_b is a fundamental characteristic of every baryon. It provides us with a simple, elegant and sensitive way for testing the validity of the theoretical hadron description in the non-perturbative sector of QCD. This includes quark soliton models, the standard quark models, various effective Lagrangians and lattice QCD calculations. μ_b provides a valuable addition to the nuclear structure functions which are being probed with very high energy leptons, giving us a snapshot of the structure of the proton. μ_b depends on the quark correlations which are not measured in the lepton experiments. The μ_b of long lived particles is measured by precession in a B-field. This technique has been used to obtain the μ of p, n, Λ, *etc.* However the short mean-life of the Δ resonance precludes using this method. Instead we can take advantage of the very short lifetime (which implies a large width) by having the Δ radiatively decay to itself. This method has been successfully pioneered for the Δ^{++} using the reaction $\pi^+ p \to \Delta^{++} \to \gamma' \Delta^{++} \to \gamma' \pi^+ p$ [1].

We propose to determine $\mu_b[\Delta^+(1232)]$ using radiative π^0 photoproduction:

$$\gamma p \to \Delta^+ \to \gamma' \Delta^+ \to \gamma' \pi^0 p \tag{1}$$

The theoretical aspects have been dealt with in detail already by the theory groups at MAMI [2] and Tuebingen [3]. μ can be determined from the differential cross section $d\sigma^5/d\Omega_\gamma d\Omega_\pi dE_\gamma$ and from the asymmetry, Σ, for linearly polarized photons.

The cross section is small ($\sigma \sim 60$ nb [4]) so we need an intense, tagged, linearly polarized, clean photon beam for E_γ from 300 to 500 MeV. This is available at MAMI-B using the Glasgow tagger and a diamond crystal as radiator to produce linearly polarized photons via coherent bremsstrahlung. We also need a large acceptance multiphoton spectrometer which is supplied by the Crystal Ball using TAPS as a forward wall detector. The detection feasibility has already been proven by TAPS which has reported that the reaction $\gamma p \to \gamma' \pi^0 p$ can be cleanly detected [4], see Appendix G. Furthermore the CB has identified the $\pi^- p \to \gamma' \pi^0 n$ reaction with good separation from background, see App. H. The running time needed is some 500 hours for 2.5×10^5 radiative π^0 photoproduction events. The bringing into operation of the CB at MAMI and performing a test measurement is expected to require an engineering run of 300 hours. Background and empty target measurements will require another 100 hours.

References

[1] B. Nefkens *et al.,* Phys. Rev. D18, 3911 (1978).

[2] D. Drechsel and M. Vanderhaeghen, Phys. Rev. C64, 065202 (2001).

[3] A.I. Machavariani and Amand Faessler, arXiv:nucl-th/0202060 (2002).

[4] M. Kotulla, NSTAR2001 proceedings Mainz 2001, V. Metag, private communication.

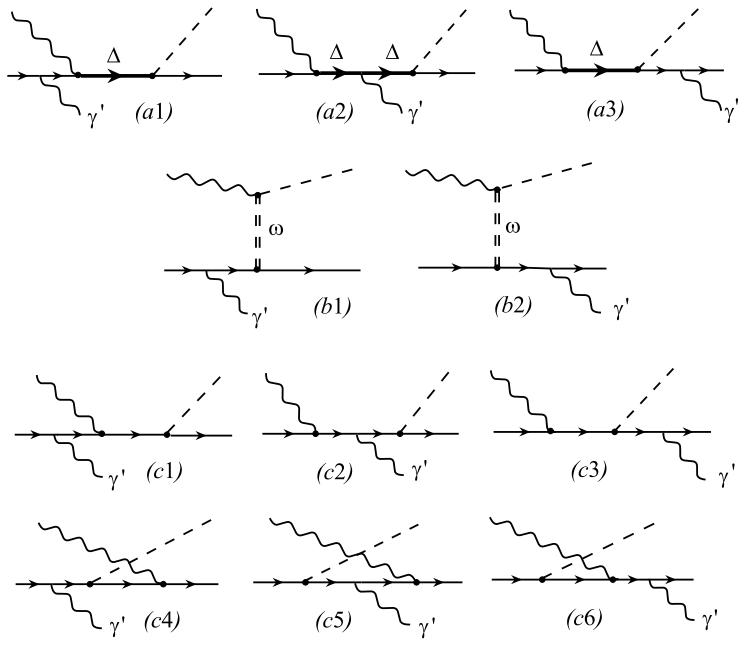

Figure 1: Feynman-diagrams for the $\gamma p \to \gamma' \pi^0 p$ reaction in the $\Delta(1232)$ region.

2 Theory: $\Delta(1232)$ static magnetic dipole moment

The static properties of baryons provide an important test for theoretical descriptions in the non-perturbative domain of QCD. In particular quark-models, chiral quark soliton models, and lattice QCD calculations give different predictions for the magnetic moment of the baryons.

The experimental values for the magnetic moments of the ground state of the baryon octet $(N, \Lambda, \Sigma, \Xi)$ are known accurately through spin precession measurements. For decuplet baryons, only the magnetic moment of the Ω^- could be determined through such techniques, because the other decuplet baryons have too short lifetimes.

The magnetic dipole moment of the $\Delta(1232)$ resonance is of considerable theoretical interest. If SU(6) symmetry holds, then the nucleon and the Δ resonance are degenerate and their magnetic moments are related through $\mu_\Delta = e_\Delta \, \mu_p$, where e_Δ is the Δ electric charge, and μ_p the proton magnetic moment. However, different theoretical models predict considerable deviations from the SU(6) value.

Some time ago it was proposed to determine the magnetic moment of the $\Delta^{++}(1232)$ by measuring the $\pi^+ p \to \gamma' \pi^+ p$ reaction [1], and the first dedicated experiment of this type was performed in the '70s [2]. As a result of these measurements and by using different theoretical analysis, the PDG [3] quotes the range : $\mu_{\Delta^{++}} = 3.7 - 7.5 \, \mu_N$ (where μ_N is the nuclear magneton), while SU(6) symmetry results in the value $\mu_{\Delta^{++}} = 5.58 \, \mu_N$. The large uncertainty in the extraction of $\mu_{\Delta^{++}}$ from the data is due to model dependence of non-resonant contributions to the $\pi^+ p \to \gamma' \pi^+ p$ reaction from the of bremsstrahlung of the charged pion (π^+) and proton (p).

As an alternative method, it has been proposed [4] to determine the magnetic moment of the $\Delta^+(1232)$ through measurement of the $\gamma p \to \gamma' \pi^0 p$ reaction, and calculations for this reaction have recently been performed in [5, 6]. Due to the small cross sections for this

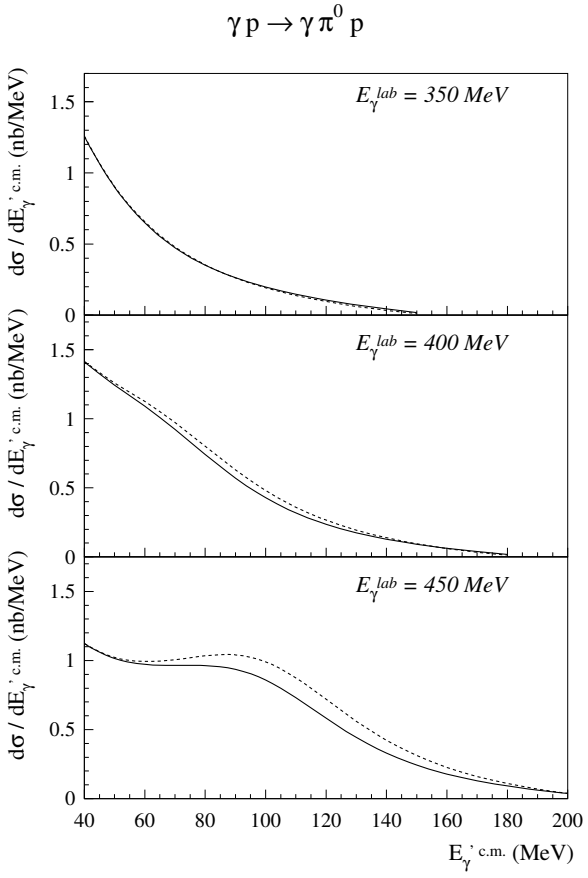

Figure 2: Energy dependence ($d\sigma/dE_\gamma^{'c.m.}$) of the outgoing photon for the $\gamma p \to \gamma' \pi^0 p$ cross section integrated over photon and pion angles. The calculations correspond to the diagrams of Fig. 1 for the values : $\kappa_{\Delta+} = 0$ (dashed curves) und $\kappa_{\Delta+} = 3$ (full curves).

reaction, which is proportional to $\alpha_{em}^2 = 1/(137)^2$, a first measurement has only now been performed by the A2/TAPS collaboration at MAMI [7]. A new experiment was proposed at ELSA with the Crystal Barrel detector [8].

To interpret the $\gamma p \to \gamma' \pi^0 p$ reaction in the $\Delta^+(1232)$ region, and to extract the value of the Δ^+ magnetic moment from it, detailed calculations have been performed in Ref. [9] which include the mechanisms represented in Fig. 1.

The diagrams shown in Fig. 1 are obtained by coupling a photon in a gauge invariant way to the mechanisms which describe the $\gamma p \to \pi^0 p$ reaction in the $\Delta(1232)$ region. This yields the Δ-diagrams (a1-a3), Born diagrams where the photon is emitted from all proton lines (c1-c6), and the vector-meson (in particular ω-meson) exchange diagrams (b1-b2) which are important at the higher energies. In these calculations, the Δ-resonance is described by a pole in the complex energy plane at the position W = $(1210 - 50\,i)$ MeV. This description of the Δ intermediate state, see Fig. 1 (a1 - a3), through a pole (without energy dependence of the pole mass and width) is important to guarantee gauge invariance [10]. In comparison with the $\gamma p \to \pi^0 p$ reaction, the description in Ref. [9] of the $\gamma p \to \gamma' \pi^0 p$ reaction invokes only one new parameter, entering the $\gamma\Delta\Delta$ vertex (a2). This new parameter is the Δ^+ anomalous magnetic moment $\kappa_{\Delta+}$. The Δ^+ magnetic moment $\mu_{\Delta+}$ is then obtained as : $\mu_{\Delta+} \equiv (1 + \kappa_{\Delta+})\, e/(2M_\Delta) = (1 + \kappa_{\Delta+})\, M_N/M_\Delta\, \mu_N$, where M_N (M_Δ) represent the mass of

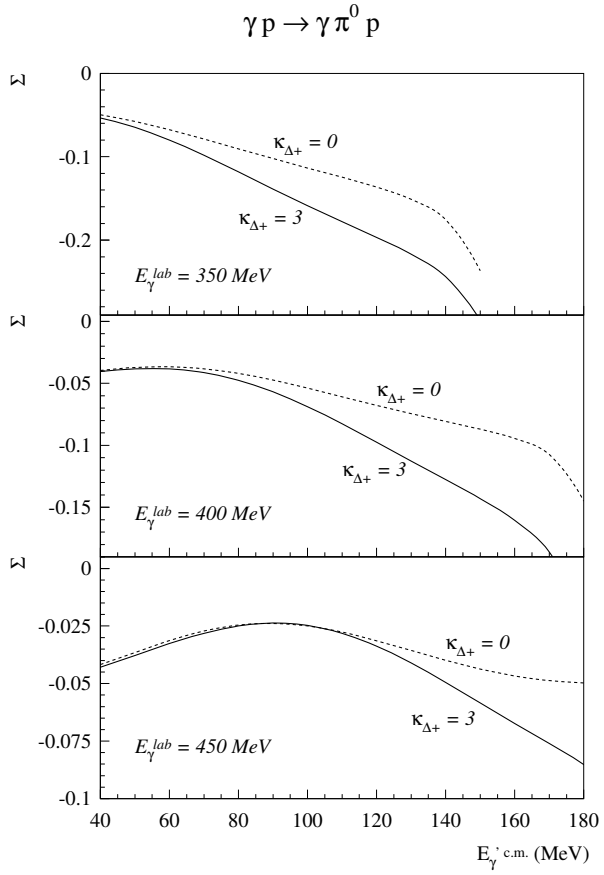

Figure 3: Outgoing photon c.m. energy dependence of the $\gamma p \to \gamma' \pi^0 p$ photon asymmetry $\Sigma \equiv (d\sigma_\perp - d\sigma_\parallel)/(d\sigma_\perp + d\sigma_\parallel)$, partially integrated over the photon and pion angular range $0^o < \theta_\gamma^{c.m.} < 90^o$, $0^o < \theta_\pi^* < 180^o$, $-90^o < \Phi_\pi^* < 90^o$, and differential w.r.t. the outgoing photon energy $E_\gamma^{'c.m.}$. The calculations are the total results, corresponding to all diagrams of Fig. 1), for the values : $\kappa_{\Delta+} = 0$ (dashed curves) and $\kappa_{\Delta+} = 3$ (full curves).

$N(\Delta)$.

In Fig. 2 we show the results of these calculations for the $\gamma p \to \gamma' \pi^0 p$ cross sections and compare them to the preliminary, very first data of the TAPS Collaboration [7] which have been obtained at the MAMI accelerator. The cross sections in Fig. 2 which have been, integrated over all pion and photon angles, are dominated by the bremsstrahlung contributions where the photons are emitted around the proton directions. This leads to the typical $1/E_\gamma^{'}$ energy dependence of the cross sections at the smaller values of the energy $E_\gamma^{'}$ of the emitted photon. One also clearly sees a qualitative change of the shape of the theoretical cross sections in the Δ region, in agreement with the trend of the preliminary data. Fig. 2 shows that the sensitivity of these integrated data to the magnetic moment of the Δ is of the order of 10-20 %, which is of the same size as the present experimental errors.

The sensitivity to the Δ magnetic moment of the integrated data of Fig. 2 can be enhanced by using a polarized photon beam. This is illustrated in Fig. 3, where the photon asymmetry $\Sigma \equiv (d\sigma_\perp - d\sigma_\parallel)/(d\sigma_\perp + d\sigma_\parallel)$ is shown, integrated over photon and pion angles, as in Fig. 2. In comparison with the unpolarized cross section, one clearly has a larger sensitivity to the Δ magnetic moment especially at the higher energies of the outgoing photon.

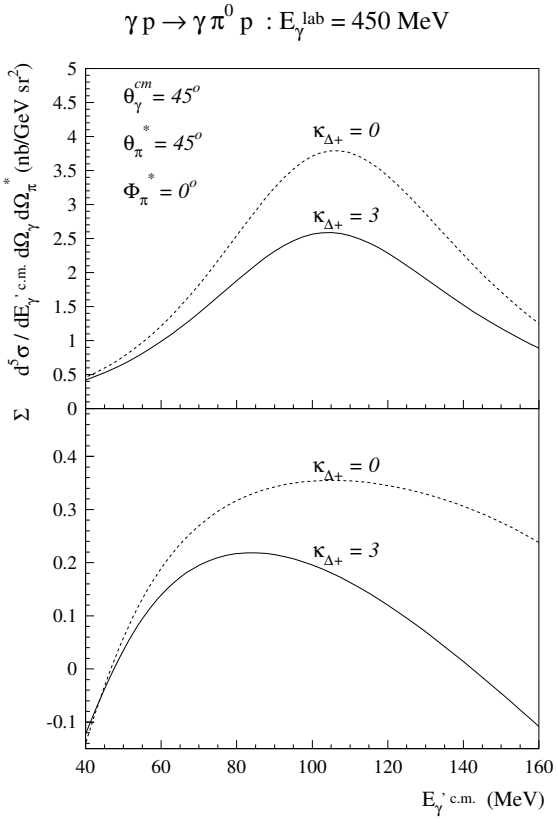

Figure 4: Five-fold differential cross section $d^5\sigma$ (upper panel), and corresponding photon asymmetry Σ (lower panel) for the $\gamma p \to \gamma' \pi^0 p$ reaction as function of the outgoing photon c.m. energy. The calculations are the total results (including all diagrams of Fig. 1), for the two values of $\kappa_{\Delta+}$ as indicated on the curves.

The sensitivity of the $\gamma p \to \gamma' \pi^0 p$ reaction on the Δ magnetic moment can be further enhanced by measuring more differential cross sections. By selecting an angular range where the photon is emitted in the backward hemisphere with respect to both protons (in the c.m. system), one can suppress the bremsstrahlung contributions and enhance the sensitivity of this reaction to κ_Δ, as shown e.g. in Fig. 4. The figure shows that the maximum of the differential cross sections for $\kappa_\Delta = 0$ is reduced by about 30 % compared to the value for $\kappa_\Delta = 3$. Also in the photon asymmetry the difference between both theoretical values is further enhanced.

A dedicated experiment using a 4π detector and a high intensity polarized photon beam, promises to provide a good opportunity to extract the Δ^+ magnetic dipole moment from the $\gamma p \to \gamma' \pi^0 p$ reaction.

In view of the anticipated very precise experimental data, one needs to further refine the theoretical description and study the error on the extraction of κ_Δ due to the theoretical model to describe the $\gamma p \to \gamma' \pi^0 p$ reaction. In particular the rescattering (unitarity) corrections of the produced particles in this process have to be estimated. Those have been neglected in the tree-level diagram based calculation of Fig. 1. At present, these corrections are being evaluated within a dynamical model [11].

One may also envisage to extend the method to extract the magnetic moment of other resonances. Of particular interest is the magnetic moment of the $S_{11}(1535)$ resonance which

could be studied through the $\gamma p \to \gamma' \eta p$ reaction. A calculation of the latter reaction, along the same way as for the $\gamma p \to \gamma' \pi^0 p$ reaction outlined above, is underway [11].

References

[1] L. A. Kondratyuk und L. A. Ponomarov, Yad. Fiz. 7 (1968) 11. [Sov. J. Nucl. Phys. 7 (1968) 82].

[2] B. M. K. Nefkens *et al.*, Phys. Rev. D 18, 3911 (1978) 3911.

[3] D. E. Groom *et al.*, Eur. Phys. J. C 15 (2000) 1.

[4] Finanzierungsantrag SFB 201 (1984-86), S. 56.

[5] A. I. Machavariani, A. Faessler, and A. J. Buchmann, Nucl. Phys. A 646 (1999) 231.

[6] D. Drechsel, M. Vanderhaeghen, M. M. Giannini, E. Santopinto, Phys. Lett. B 484 (2000) 236.

[7] M. Kotulla, PhD thesis, Giessen University (Germany), 2001.

[8] R. W. Gothe *et al.*, *Inelastic Photon Scattering in the Exclusive Channels* $p(\gamma\pi^0\gamma p)$ *and* $p(\gamma\eta\gamma p)$ Proposal to the ELSA/MAMI PAC (2001).

[9] D. Drechsel and M. Vanderhaeghen, Phys. Rev. C 64 (2001), 065202.

[10] G. López Castro and A. Mariano, hep-ph/0010045.

[11] W.-T. Chiang *et al.*, in preparation.

3 Experiment: $\Delta(1232)$ static magnetic dipole moment

We propose to use the Crystal Ball multiphoton spectrometer as the central detector with the TAPS as forward wall for the detection of the photons. This combination has a geometrical acceptance close to 4π, a high photon detection efficiency with excellent energy and angular resolutions. The polar and azimuthal angles of the outgoing proton for $\Theta_{lab} > 20^\circ$ will be measured by a central tracker based on the DAPHNE cylindrical multiwire proportional chamber. The chamber will be inserted into the Crystal Ball beam cavity. The trajectory and energy of the proton for $\Theta_{lab} < 20^\circ$ will be measured by the TAPS forward wall. The experimental apparatus is shown in Fig. 5. The detailed description of the Crystal Ball, the TAPS forward wall, the cylindrical wire chamber, and the liquid hydrogen target is given in Appendices C, D, E, and F.

The overall efficiency of the experimental apparatus for the reaction $\gamma p \to \pi^0 \gamma p$ at an incident beam energy of $E_\gamma = 400$ MeV is shown in Fig. 6. The distributions have been obtained with a GEANT based Monte Carlo simulation code developed for the experiments with the Crystal Ball at MAMI. The code includes a detailed description of the Crystal Ball detector as well as a description of the TAPS forward wall, the central tracker and the liquid hydrogen target. The analysis of the Monte Carlo data is performed with the Analyzer software package initially developed for the Crystal Ball AGS experiments. The Analyzer

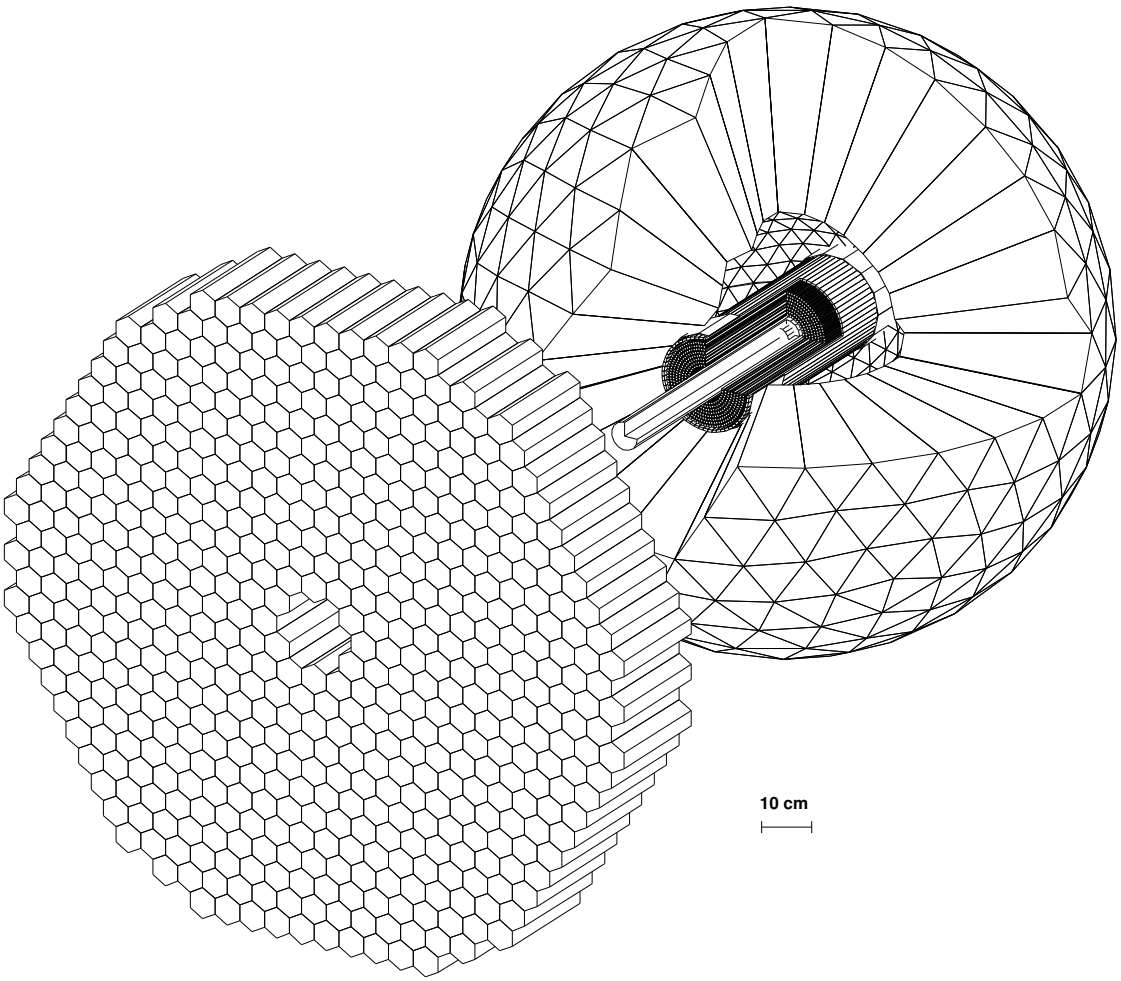

Figure 5: The experimental apparatus proposed for the measurements of $\mu_b[\Delta^+(1232)]$ at MAMI. To show the position of the cylindrical wire chamber and the target inside the Crystal Ball some of the Crystal Ball crystals have been omitted. The central detector, the Crystal Ball, TAPS as forward wall, the cylindrical wire chamber, and the liquid hydrogen target are described in Appendices C, D, E, and F.

modified for the MAMI experiments includes a TAPS cluster recognition routine as well as track reconstruction in the cylindrical wire chamber. The acceptance is shown for events in which all three photons are detected and the direction of the recoil proton is measured.

The expected $\gamma p \to \gamma' \pi^0 p$ total cross section is ~ 60 nb (see App. G). The reaction has three photons and one proton in the final state. At an incident beam energy of $E_\gamma = 400$ MeV the energy of the photons from π^0 decay ("decay" photons) are distributed from 10 to 370 MeV. The single photon produced in the reaction ("production" photon) has an energy spectrum from 0 to 250 MeV with the maximum at about 100 MeV for a uniform Dalitz plot. The outgoing proton kinetic energy varies between 0 and 170 MeV with the high energy protons always going forward. The thickness of both detectors is enough to stop the proton which makes the measurement of the proton energy possible. The anticipated background

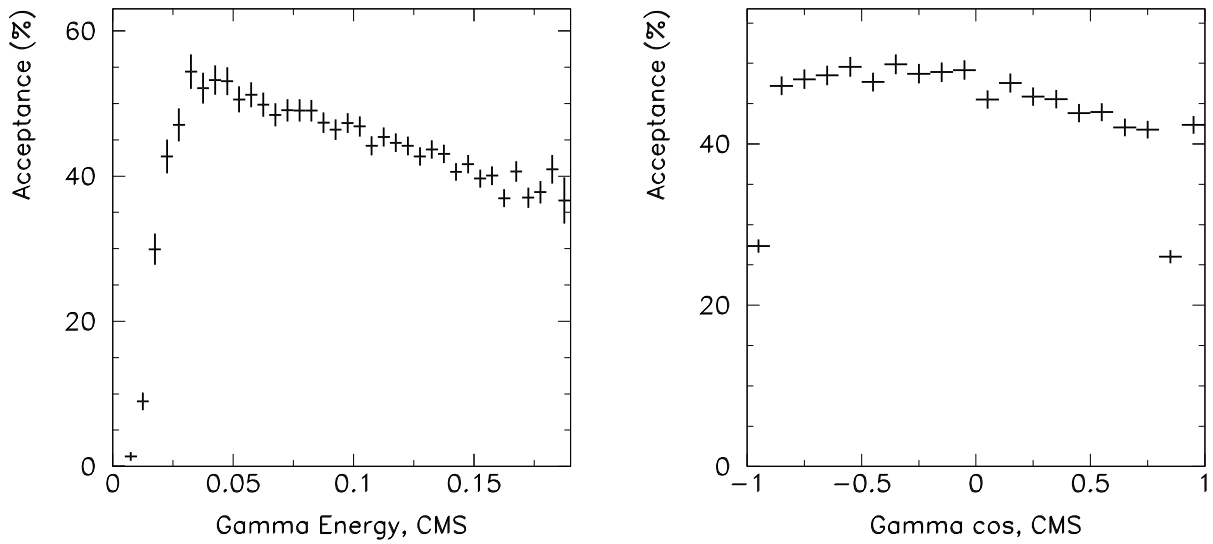

Figure 6: The Monte Carlo simulation of the overall acceptance of the experimental apparatus shown in Fig. 5. Results are shown for the reaction $\gamma p \to \gamma' \pi^0 p$ for an incident beam energy of 400 MeV. The acceptance is shown for the events for which all three photons are detected and the direction of the recoil proton is measured.

reactions are

$$\gamma p \to \pi^0 p, \tag{2}$$

$$\gamma p \to \pi^0 \pi^0 p, \tag{3}$$

Reaction 2 at our incident photon energy has a total cross section of about 150 μb [1]. It will contribute into the "good" events sample due to cases where one of the decay photons has produced two clusters in a photon detector ("split-off"). When the energy in one of the clusters is close to the energy of the original photon the invariant mass of the π^0 is reconstructed. The extra low-energy cluster then will simulate the production photon. The Monte Carlo shows that the extra cluster has a typical energy of 20 MeV, see Fig. 7. This background will be suppressed by about a factor of 1000 by applying a cut on the energy of the production photon of 50 MeV. An information on the trajectory and the energy of the outgoing proton will be used for an additional suppression of the background.

The $\gamma p \to \pi^0 \pi^0 p$ reaction has a total cross section of 100 nb [2]. It has four photons in the final state contributing to the good events candidates if one of the photons is not detected. A high geometrical acceptance and detection efficiency for photons is required in order to suppress this background. The measured trajectory of the outgoing proton will also provide an important constraint on the missing momentum of the reaction which allows us to separate the background events. A factor of 100 suppression was achieved for this background type in the analysis of our Monte Carlo data, see Fig. 8.

The simplest trigger conditions for the experiment require a coincidence between energy-sum-signals of the NaI counters of the CB and the BaF_2 counters of the TAPS detector. The expected event rate of 2.5 KHz is mainly determined by $\gamma p \to \pi^0 p$ and $\gamma p \to \pi^+ n$ processes. The contribution of $\gamma p \to \pi^+ n$ can be decreased by optimizing the threshold

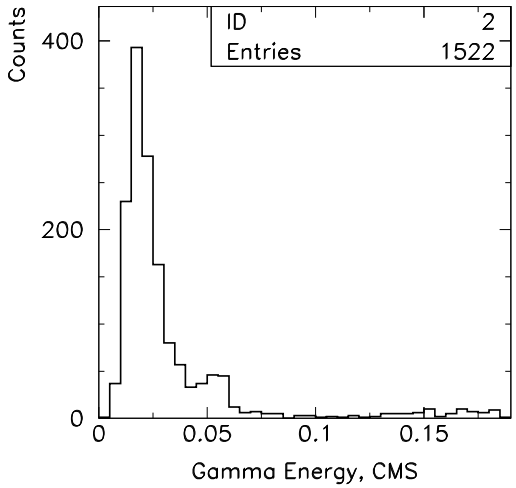

Figure 7: The energy spectrum of the production photon for the $\gamma p \to \pi^0 p$ background reaction. The extra low-energy photon appears in the cases when one of the decay photons has produced two clusters in a photon detector ("split-off"). The result of the Monte Carlo is shown for 10^5 initially generated $\gamma p \to \pi^0 p$ events.

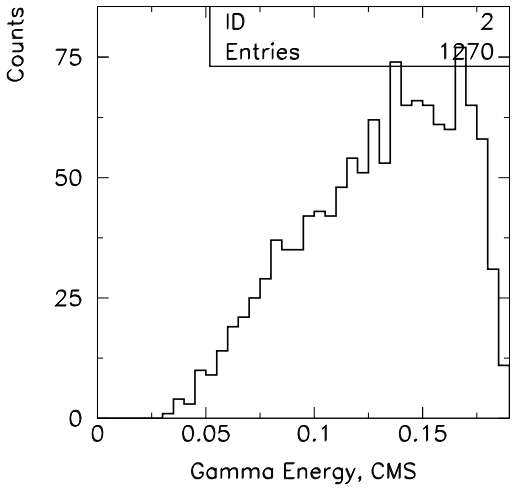

Figure 8: The Monte Carlo results for the energy spectrum of the production photon for the $\gamma p \to \pi^0 \pi^0 p$ background reaction. 10^5 $\gamma p \to \pi^0 \pi^0 p$ events were initially generated.

applied to the total energy of the the photon detectors. The implementation for the new Crystal Ball and TAPS readout electronics is underway [4]. The anticipated readout speed for the new data acquisition system is 1 KHz plus. Additional trigger conditions will be applied if necessary in order to keep the event rate under 1 KHz and the data acquisition system live time above 70%. The proposed algorithm utilizes a block of fast logic matrices to analyze the pattern of crystals in both photon detectors. The pattern recognition unit provides information on the number of clusters in the detectors within 300 nsec after an event is detected. The algorithm as well as the electronics hardware have been developed at the University of Uppsala (Sweden) for the WASA experiment [3].

4 Event Rates

The proposed experiment will use the MAMI/Glasgow Tagged Photon beam in the MAMI A2 area that has been used successfully for many years.

The parameters entering the count rate estimate and resulting beam time request are:

- Incoming electron beam energy: $E_0 = 882$ MeV.
- Tagged photon energy range: $E_\gamma^t = 295 - 820$ MeV.
- Electron count rate in the tagger: $N_e = 5 \times 10^5 \ \frac{1}{s \ MeV}$.
- Tagging efficiency: $\varepsilon_t \approx 50\%$.

- Tagged photon flux: $N_\gamma = 2.5 \times 10^5 \ \frac{1}{s \ MeV}$.
- Number of protons in a 5 cm long LH_2 target (existing DAPHNE cryo target): $N_t = 2.1 \times 10^{23} \ \frac{1}{cm^2}$.
- Detection efficiency: $\varepsilon_{CB} \approx 40\%$. (see Fig. 6).
- Data acquisition system live time: $\varepsilon_{DA} \approx 70\%$.
- Total cross section $\gamma p \to \gamma' \pi^0 p$: $\sigma_t \sim 60$ nb (see Fig. 26).
- Differential cross section: $d\sigma/dE'_\gamma \sim 0.5$ nb/MeV. (see Fig. 2).

The resulting number of events expected per hour per MeV of the incident photon energy and per MeV of production photons is

$$N_{\gamma\prime} = N_\gamma \ \frac{d\sigma}{dE'_\gamma} \ N_t \ \varepsilon_{CB} \ \varepsilon_{DA} \approx 0.03 \ \Big[\frac{1}{MeV} \ \frac{1}{h} \ \frac{1}{MeV}\Big]. \tag{4}$$

The beam time requested for the data taking is 500 hours, also 300 hours for an engineering run plus 100 hours for empty target and background measurements. This will provide about 2.5×10^5 $\gamma p \to \pi^0 \gamma p$ events integrated over the production photon energy of $E'_\gamma = 30 - 150$ MeV and over a 150 MeV region between 340 and 490 MeV for the tagged incident photons. About half of the events will have the production photon energy in the c. m. above 70 MeV. This part of the spectra is most sensitive to the magnetic dipole moment.

The expected rate for the differential cross section over ± 25 MeV incident photon energy and ± 10 MeV production photon energy is

$$N_{\gamma\prime} \approx 26.5 \ \Big[\frac{1}{50 \ MeV} \ \frac{1}{h} \ \frac{1}{20 \ MeV}\Big]. \tag{5}$$

The rate is a factor of 500 higher compared to the one which has been obtained in the TAPS experiment (see Appendix G).

The photon asymmetry Σ will be measured with the coherent peak set at about 450 MeV. The linearly polarized photons will cover the energy range between 370-450 MeV with the mean polarization of $p_\gamma \approx 40\%$. The number of events expected in the 500 hours is about 1.3×10^4 per bin of ± 25 MeV incident photon energy and ± 10 MeV production photon energy. The expected accuracy in the photon asymmetry is

$$\Delta\Sigma = \frac{1}{p_\gamma} \ \frac{1}{\sqrt{N}} \approx 0.02 \tag{6}$$

per bin of $E^t_\gamma = \pm 25$ MeV and $E'_\gamma = \pm 10$ MeV.

References

[1] M. McCormick *et al.*, Phys. Rev. C **53**, 41 (1996).

[2] M. Wolf *et al.*, Eur. Phys. J. A **9**, 5 (2000).

[3] P. Marciniewski: http://www.tsl.uu.se/ pawel/, Feb. 2002.

[4] R. Beck *et al.* CB@MAMI-3-2002, internal report at http://bmkn8.physics.ucla.edu/Crystalball/Docs/documentation.html (2002).

[5] D. Drechsel, M. Vanderhaeghen, M. M. Giannini, E. Santopinto, Phys. Lett. B **484**, 236 (2000).

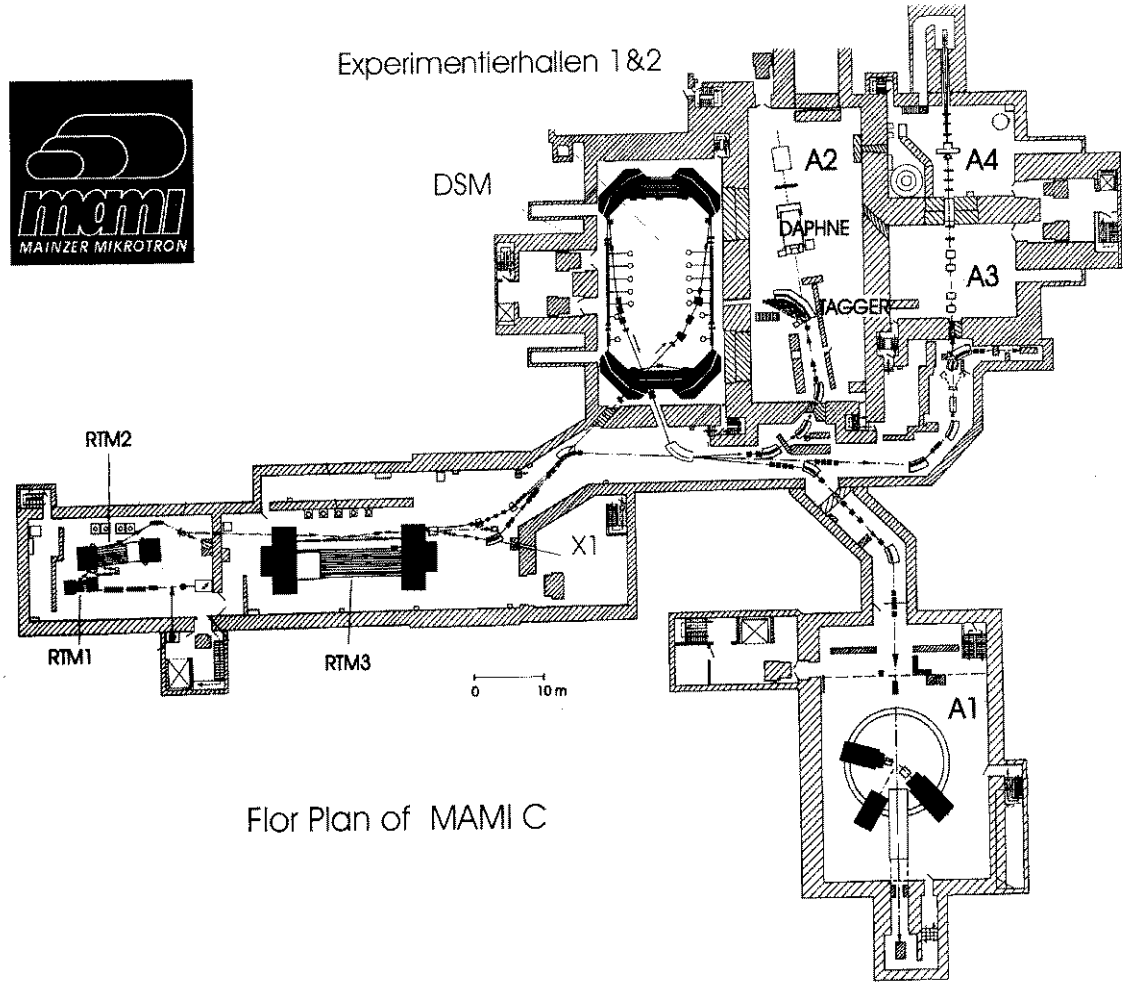

Figure 9: The MAMI facility. The beamline components and all four experimental areas are shown. It is planned that the Crystal Ball occupies experimental area A2.

A The MAMI Facility

MAMI is a multistage electron accelerator with a maximum electron energy of 855 MeV and a duty cycle of 100%. Figure 9 shows a schematic of the MAMI floor plan. We plan to install the Crystal Ball in experimental area A2, shown in detail in Fig. 10. This area is currently occupied by the DAPHNE detector.

The electrons have an initial energy of E_0. Photons are created via bremsstrahlung, and the electrons are then tagged by a 353-element hodoscope, see Appendix B for details. The outgoing electron's energy, E', is measured by the tagging hodoscope, and the photon energy E_γ is calculated as

$$E_\gamma = E_0 - E' \tag{7}$$

The E' spectrum is shown in Fig. 11. For a given initial electron energy E_0, the photon energy range is given by

$$0.05E_0 < E_\gamma < 0.94E_0 \tag{8}$$

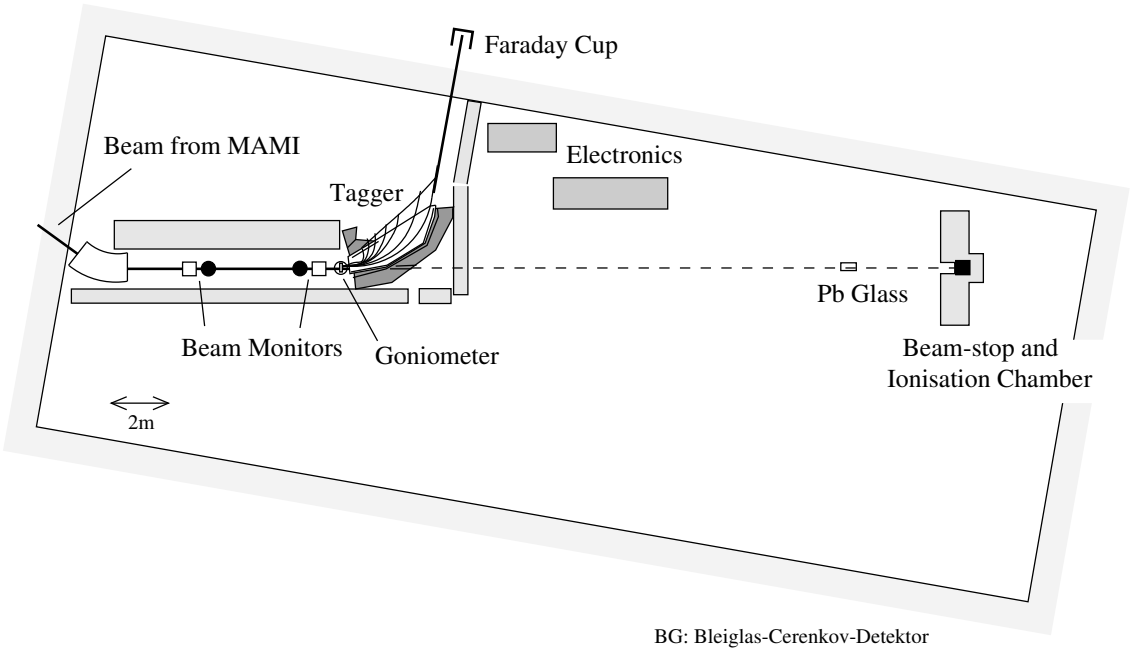

Figure 10: The A2 experimental hall at MAMI. The Crystal Ball will be in the space currently occupied by the DAPHNE detector.

The maximum tagging rate of the photon tagger is $10^8\gamma/s$. The photon tagger can produce unpolarized photons by making use of an unpolarized electron beam incident on a high-Z target such as gold. It can also produce circularly polarized photons, by using a longitudinally polarized electron beam incident on the radiator, or linearly polarized photons, by using coherent bremsstrahlung on a diamond radiator.

Linearly polarized photons with a degree of polarization up to 70% are produced by coherent bremsstrahlung from a diamond crystal[1]. To continuously monitor the photon polarization and flux, a plastic pair detector is used downstream of the target area. The photon polarization is determined from the photon spectrum measured by the tagging spectrometer in coincidence. The was tested by an absolute measurement of the photon polarization using coherent π^0 photoproduction on ^4He as a polarimeter reaction with an analyzing power $A = 100\%$. Excellent agreement between calculations and experiment was found; in this way[2], both the photon polarization and the photon flux can be determined with an absolute precision of better than $\pm 2\%$. Figure 12 shows the photon polarization for linearly polarized photons as a function of the photon energy, expressed as a fraction of the initial electron energy, E_0. Note that the maximum energy for linearly polarized photons is slightly more than $E_0/2$.

References

[1] A. Schmidt, Diplomarbeit Mainz (1995).

[2] D. Lohmann et al., Phys. Rev. C 58 (1998) 489.

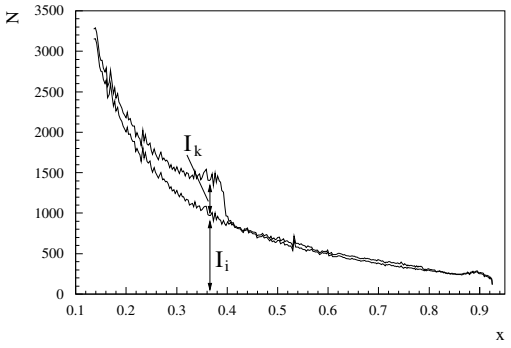

Figure 11: The E' spectrum for the tagging system in the A2 experimental hall at MAMI.

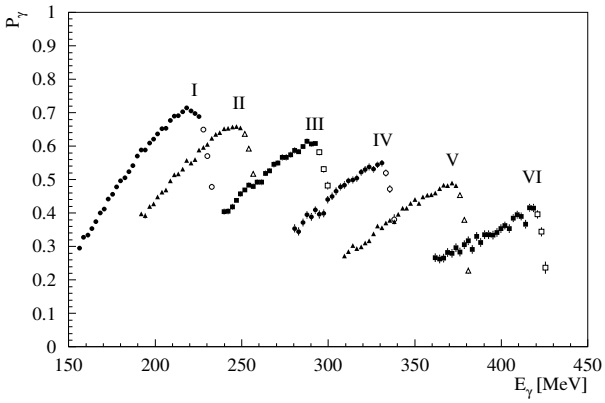

Figure 12: The photon polarization for linearly polarized photons in the A2 experimental hall at MAMI as a function of photon energy (expressed as a fraction of the initial electron's energy).

B The Glasgow Photon Tagger at MAMI

The tagging facility at MAMI B ($E_0 = 855$ MeV) allows bremsstrahlung photons in the energy range $40 - 800$ MeV to be tagged with a resolution of ~ 2 MeV at rates up to $10^8\ s^{-1}$. The system consists of a momentum-dispersing electron spectrometer, with intrinsic energy resolution of 120 KeV [1] (see Fig. 13). This spectrometer focuses post-bremsstrahlung electrons onto a focal plane where the position and time of arrival is established by a detector array [2]. This focal plane detector consists of 353 half overlapping plastic scintillators, where the overlap region between two of the detectors define the energy resolution of the tagged photon beam (~ 2 MeV at $E_0 = 855$ MeV). The maximum tagged photon flux is limited to $\sim 10^6 s^{-1}$ per single focal plane detector and to $10^8 s^{-1}$ for the full energy range $E_\gamma = 40-800$ MeV for an 855 MeV incoming electron beam. To increase the photon flux in the higher energy range, for example for the $2\pi^0$– and η–production, the focal plane detectors below the threshold energies ($E_\gamma^{th}(p2\pi^0) = 310$ and $E_\gamma^{th}(p\eta) = 710$ MeV) can be switched off.

In addition to the standard focal plane detector a high resolution device can be installed in the focal plane, which allows to increase the energy resolution and the photon flux. This device consists of 96 scintillation fibers $2 * 3$ mm^2 and 230 mm long in size, which covers an energy range of 70 MeV for $E_0 = 855$ MeV with a resolution of 360 KeV and allows to increase the tagged photon flux by a factor 2.5 [3].

References

[1] I. Anthony et al., NIM A 301 (1991) 230.

[2] S.J. Hall et al., NIM A 368 (1996) 698.

[3] A. Reiter, Diplomarbeit Mainz (1999).

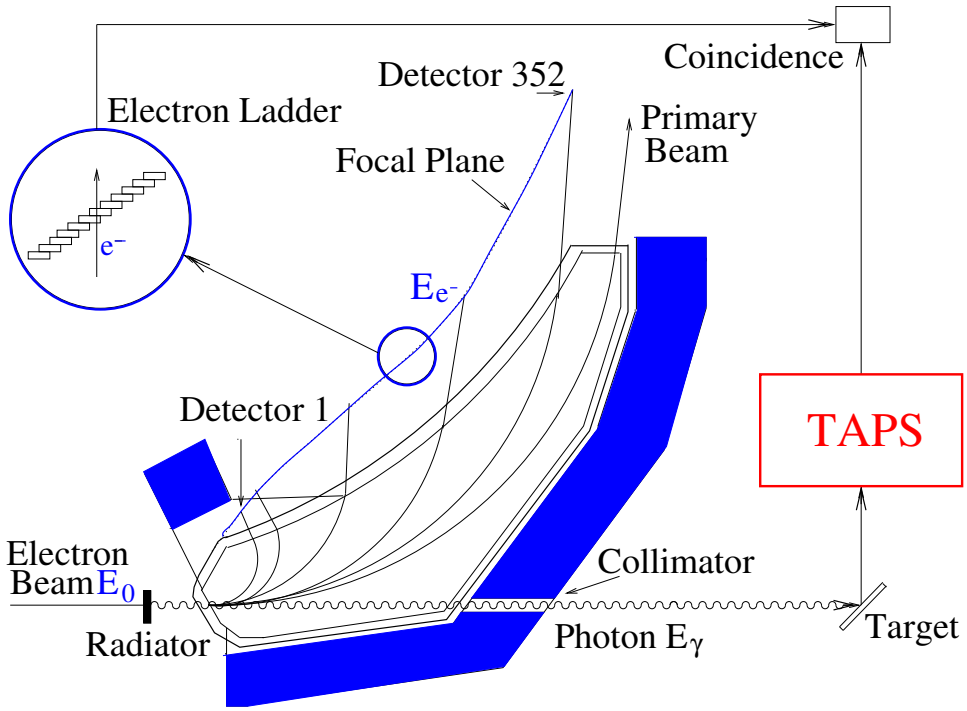

Figure 13: The photon tagger in the A2 experimental hall at MAMI.

C The Crystal Ball spectrometer

The Crystal Ball, CB, spectrometer consists of a highly segmented sphere made of NaI. The sphere has an entrance and exit tunnel for the beam and a spherical cavity for the liquid hydrogen target, see Fig.14. For the AGS experiments on baryon spectroscopy the target was surrounded by a cylinder of scintillation counters that functioned as the charged particle veto. The solid angle of the CB is 93% of 4π steradian. The Crystal Ball was build at SLAC and used in J/ψ measurements at SPEAR and b–quark physics at DESY [1, 2, 3, 4, 5].

The CB is constructed of 672 optically isolated NaI(Tl) crystals, 15.7 radiation lengths thick. The counters are arranged in a spherical shell with an inner radius of 25.3 cm and an outer radius of 66.0 cm. The hygroscopic NaI is housed in two hermetically sealed evacuated hemispheres. The CB geometry is based on that of an icosahedron. Each of the 20 triangular faces ("major triangles") is divided into four "minor triangles", each consisting of nine separate crystals. Each crystal is shaped like a truncated triangular pyramid, 40.6 cm high, pointing towards the center of the Ball. The sides on the inner end are 5.1 cm long and 12.7 cm on the far end, see Fig.14. Each crystal is individually wrapped in reflector paper and aluminized mylar; it is viewed by its own 5.1 cm diameter SRC L50 B01 photomultiplier, selected for linearity over a wide dynamic range. The phototube is separated from the crystal by a glass window and a 5 cm air gap. The crystals have been stacked so as to form two mechanically separate top and bottom hemispheres. The boundary between the two hemispheres is called the equator region. It is $\sim$ 0.8 cm thick, consisting of two 1.6 mm stainless steel plates separated by 5 mm of air. This introduces an inactive space amounting to 1.6% of the solid angle. The inner wall of the hemisphere is 1.5 mm stainless steel or 0.09 r.l. The Ball has an entrance and exit opening for the beam which results in a loss of 4.4% of acceptance. The Crystal Ball resides in a dry room for extra safeguarding in case of a leak. The dry room maintains a constant temperature of $(20 \pm 1)^{\circ}$C and a low

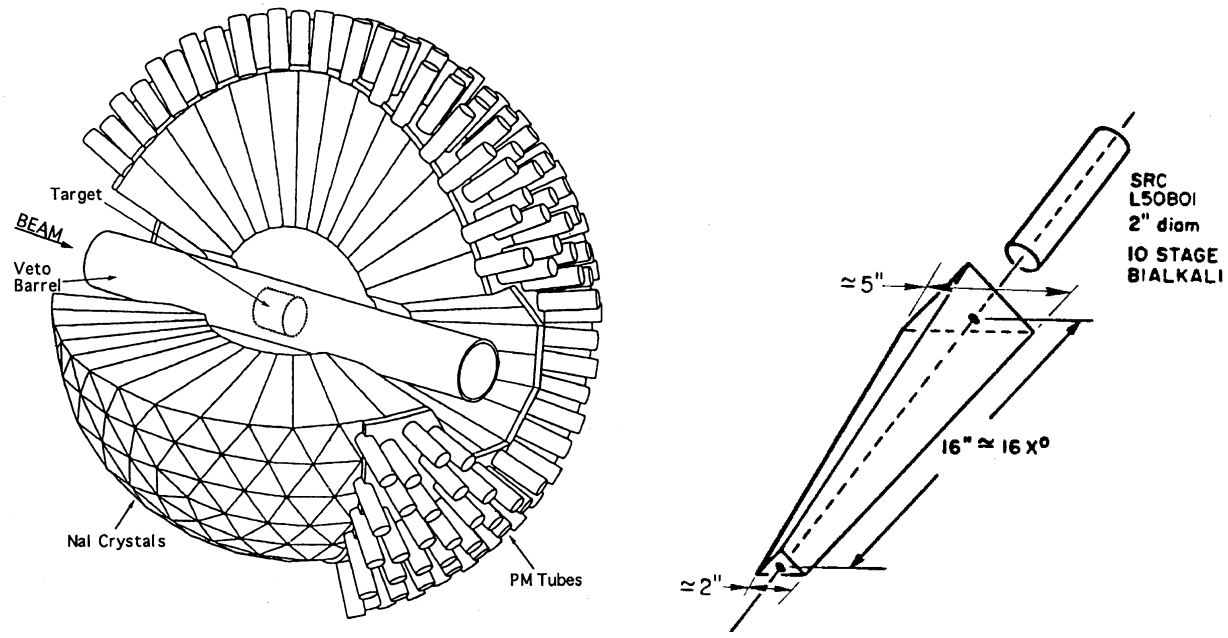

Figure 14: Left: The Crystal Ball detector. Right: Typical Crystal Ball crystal.

humidity environment. The dry room was equipped with beam entrance and beam exit mylar windows.

The Crystal Ball was moved to Brookhaven National Laboratory (BNL) at the end of 1995 in order to pursue a new extensive program in baryon spectroscopy and η physics [6, 7, 8, 9, 10].

Electromagnetic showers in the spectrometer are measured with an energy resolution $\sigma_E/E \sim 1.7\%/(E\ (\mathrm{GeV}))^{0.4}$; the angular resolution for photon showers at energies of 0.05–0.5 GeV is $\sigma_\theta = 2°$–$3°$ in the polar angle and $\sigma_\phi = 2°/\sin\theta$ in the azimuthal angle.

The initial relative hardware calibration of the crystals was made using the 0.661 MeV gammas from a ^{60}Co source. A typical spectrum obtained with the ^{60}Co source from a single crystal is shown in Fig. 15. The absolute energy calibration was done making use of the invariant mass of the $\pi^0 \to 2\gamma$ and $\eta \to 2\gamma$ and $\eta \to 3\pi^0$ processes. An example of the experimental resolution obtained in series of pion runs with a thin CH_2 target is shown in Fig. 16. The figure shows the distribution of the invariant mass for two photons obtained for the CH_2 target after subtraction of the normalized carbon and empty target data. The missing mass of the two photons was required to be the mass of the neutron. The first peak in the spectrum has the mass of the π^0, its width is $\sigma = 11.5$ MeV/c^2, it is due to $\pi^- p \to \pi^0 n$. The second peak has the mass of the η, it is due to $\pi^- p \to \eta n$ followed by the $\eta \to 2\gamma$ decay; the width of the η peak is $\sigma = 18.0$ MeV/c^2.

High granularity and a large acceptance makes the Crystal Ball a unique instrument to detect reactions with multiphoton final states. One of the examples of such a reaction is $\pi^- p \to \eta n$ followed by the $\eta \to 3\pi^0 \to 6\gamma$ decay. Figure 17a shows the invariant mass of the 6γ satisfying a χ^2 test for the reaction $\pi^- p \to \eta n \to 6\gamma n$. The distribution has the width of the η peak with $\sigma \approx 18.0$ MeV/c^2. The typical CB acceptance for the six photon final states is about 10%. The fact that the $\eta \to 6\gamma$ decay occurs via intermediate $3\pi^0$'s allows us to apply three additional constraints, namely the masses of the $3\pi^0$'s. Such constraints are useful to reduce a background and to improve the experimental resolution. The improved

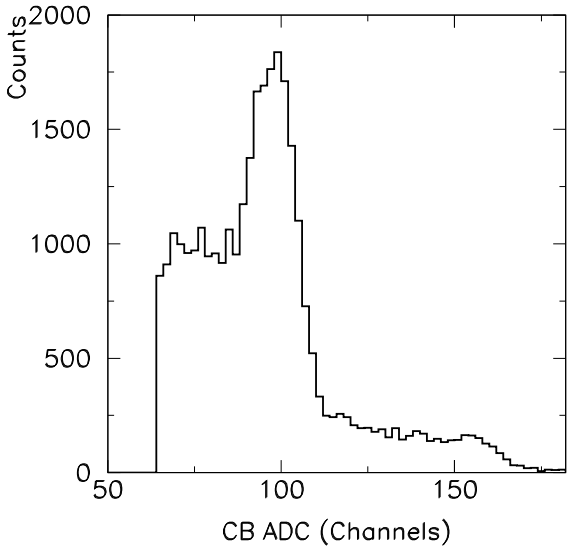

Figure 15: Typical ^{60}Co spectrum obtained from one of the CB crystals.

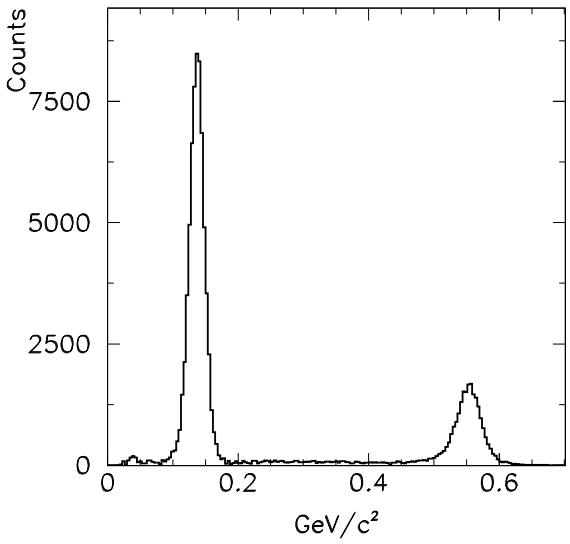

Figure 16: Invariant mass of two photons obtained with a 1.8 cm thick CH_2 target for p_{π^-}=750 MeV/c. Normalized carbon and empty target data have been subtracted. The missing mass of the two photons is required to be the mass of the neutron.

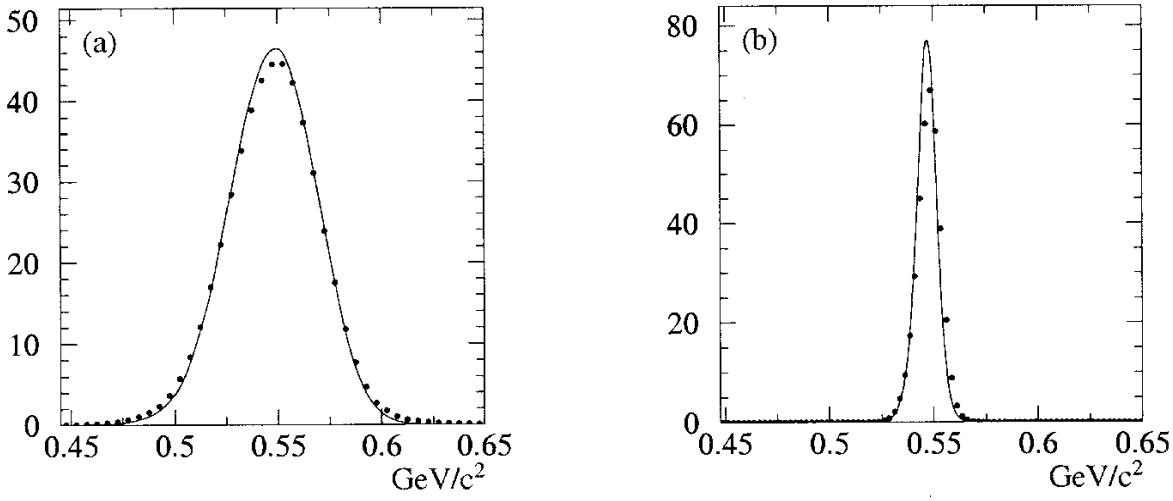

Figure 17: (a) Invariant mass spectrum for the data (dots) and Monte Carlo (line) satisfying a χ^2 test for the reaction $\pi^- p \to \eta n \to 6\gamma n$. (b) Improved resolution of (a) due to making a constrained fit to the reaction $\pi^- p \to \eta n \to 3\pi^0 n$.

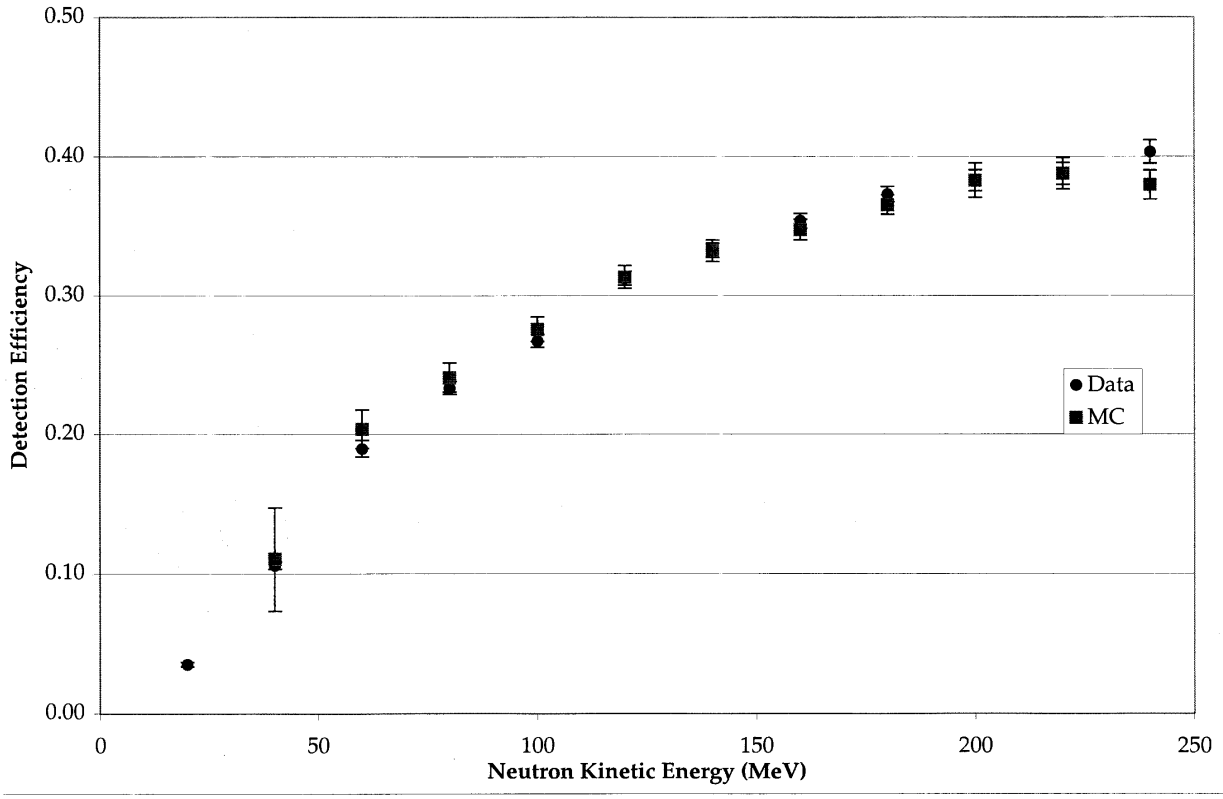

Figure 18: The neutron detection efficiency obtained with the Crystal Ball using the reaction $\pi^- p \to \pi^0 n$ for four π^- beam momenta [10].

mass resolution when applying a constrained fit to the reaction $\pi^- p \to \eta n \to 3\pi^0 n$ is shown in Fig. 17b. The width of the η peak is $\sigma \approx 5.0$ MeV/c^2. The background under the peak is estimated to be less than 1%.

The CB detects neutrons with an efficiency of $\sim$ 35% at $E_n = 150$ MeV, see Fig. 18. The thickness of the individual NaI counter is enough to stop 233 MeV $\mu^\pm$, 240 MeV $\pi^\pm$, 341 MeV $K^\pm$, or 425 MeV protons.

The CB has been successfully used for extensive studies of hyperon production: Λ is measured via $\Lambda \to \pi^0 n$, Σ^0 via $\Sigma^0 \to \Lambda\gamma$ and K_s^0 via $K_s^0 \to 2\pi^0$ decay. Figure 19 shows the decay-distance distribution of the Λ from $K^- p \to \eta\Lambda$. The experimental result for 750 MeV/c K^- is shown by the solid line. The Monte Carlo simulation is shown by the dashed line. The Λ decay distance used for the Monte Carlo is $c\tau = 7.89$ cm [7].

The anticipated MAMI rate for the beam related accidental background events calculated for each individual Crystal Ball crystal is shown in Fig. 20. The Monte Carlo results are shown for a 5 cm long liquid hydrogen target for five different thresholds.

References

[1] E.D. Bloom and C.W. Peck, Ann. Rev. Nucl. Sci. **33**, 143 (1983).

[2] H. Marsiske *et al.*, Phys. Rev. D **41**, 3324(1990).

[3] D. Antreasyan *et al.*, Phys. Rev. D **36**, 2633 (1987).

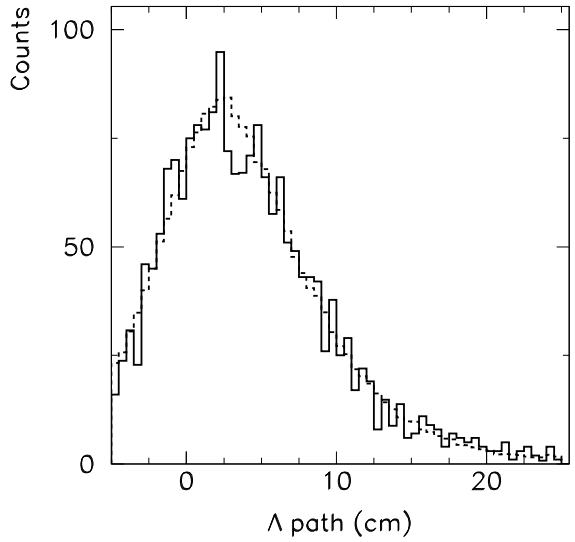

Figure 19: The decay–distance distribution of the Λ in $K^- p \to \eta\Lambda$. The experimental result for 750 MeV/c momentum kaon beam is shown by the solid line. The Monte Carlo simulation is shown by the dashed line. The Λ decay distance used for the Monte Carlo is $c\tau = 7.89$ cm [7].

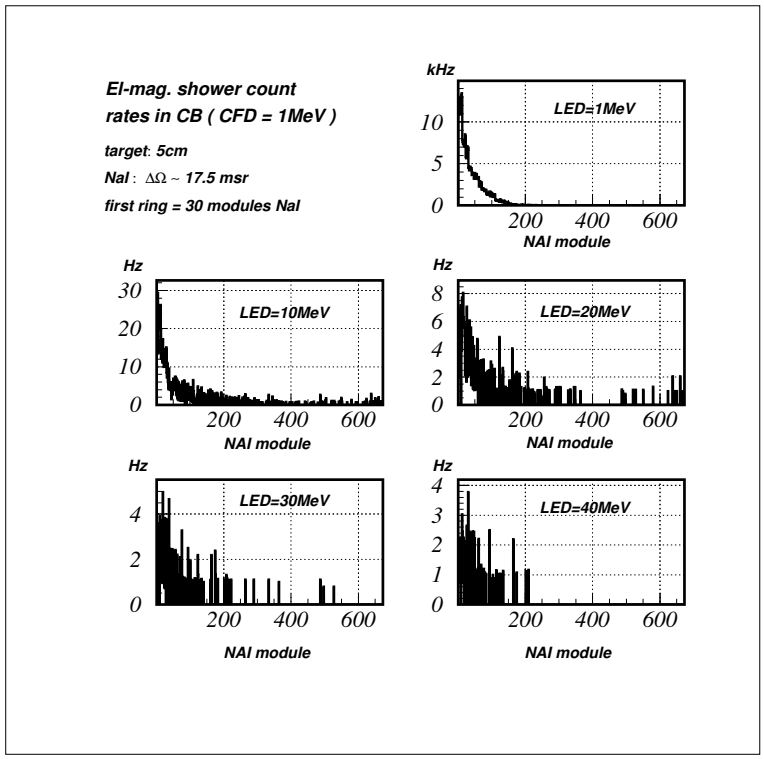

Figure 20: The rate for the beam related accidental background events calculated for each individual Crystal Ball crystal. The Monte Carlo results are shown for 5 cm long liquid hydrogen target for five different thresholds.

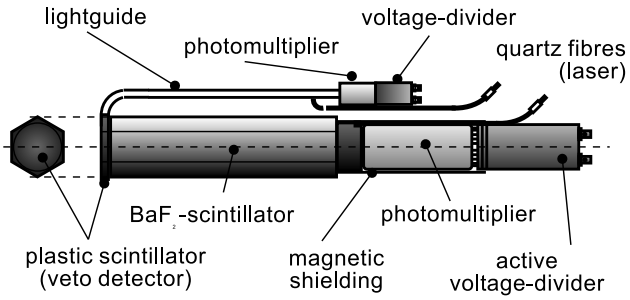

Figure 21: An individual TAPS detector.

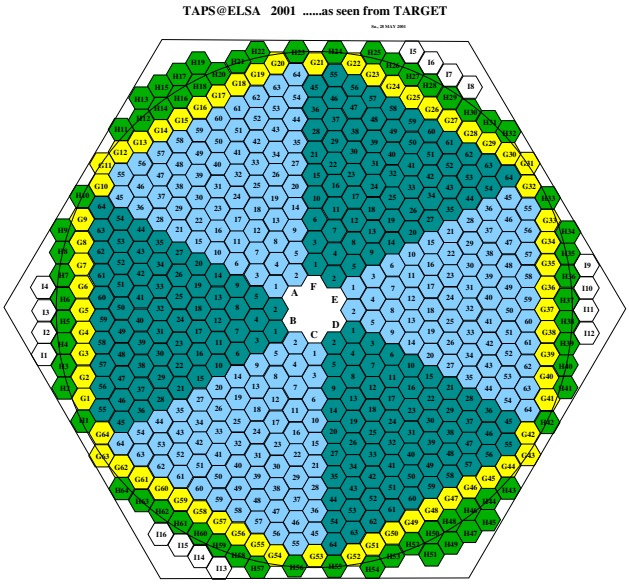

Figure 22: TAPS Forward Wall.

[4] J.E. Gaiser *et al.*, Phys. Rev. D **34**, 711 (1986).

[5] M. Oreglia *et al.*, Phys. Rev. D **25**, 2259 (1982).

[6] A. Starostin *et al.*, Phys. Rev. Lett. **85**, 5539 (2000).

[7] A. Starostin *et al.*, Phys. Rev. C **64**, 055205 (2001).

[8] S. Prakhov *et al.*, Phys. Rev. Lett. **84**, 4802 (2000).

[9] W. B. Tippens *et al.*, Phys. Rev. Lett. **87**, 192001 (2001).

[10] T. D. Stanislaus *et al.*, Nucl. Instrum. Methods (**A 462) (2001).**

D The TAPS Forward Wall

In the combined setup, TAPS [1] will be implemented as a Forward Wall at a distance of 1.8 m to the target and will cover the forward opening of the Crystal Ball (20° with respect to the beam direction). In its present configuration, TAPS comprises of 528 individual BaF_2 detectors. The BaF_2 crystals are hexagonally shaped with an inner diameter of 59 mm and a length of 250 mm (corresponding to 12 radiation lengths). The thickness of the detector is sufficient to stop 180 MeV $\pi^{\pm}$, 280 MeV $K^{\pm}$, or 360 MeV protons. Each detector has its own 5 mm plastic scintillator (NE102A) in front which serves as a charged particle veto detector (Fig. 21). BaF_2 has two scintillation light components with very different decay constants τ_s=0.76 ns and τ_l=620 ns. The relative light yield which depends on the ionization density of the particle enables the use of a pulse shape analysis to discriminate between various particle species. The excellent time resolution of the TAPS detector of FWHM=0.5 ns and the long distance to the target allow an efficient TOF measurement for further particle identification. The relative energy calibration (matching of the individual detectors) is performed by measuring minimum ionizing cosmic muon radiation, while the absolute calibration is done using the invariant mass of the $\pi^\circ \to 2\gamma$ and $\eta \to 2\gamma$ processes in

	TAPS
distance to target	180 cm
coverage (7 crystals beam hole)	4° - 20°
coverage (1 crystal beam hole)	2° - 20°
angular resolution of photons (300 MeV, 1.8 m)	FWHM 0.7°
energy resolution [2]	$\frac{\sigma}{E_\gamma} = \frac{0.79\%}{\sqrt{E_\gamma}} + 1.8\%$
invariant mass resolution π°	FWHM 19 MeV
invariant mass resolution η	FWHM 45 MeV
time resolution (experiment)	FWHM 0.5 ns
neutron efficiency [3]	25 %

Table 1: Specification of the TAPS detector.

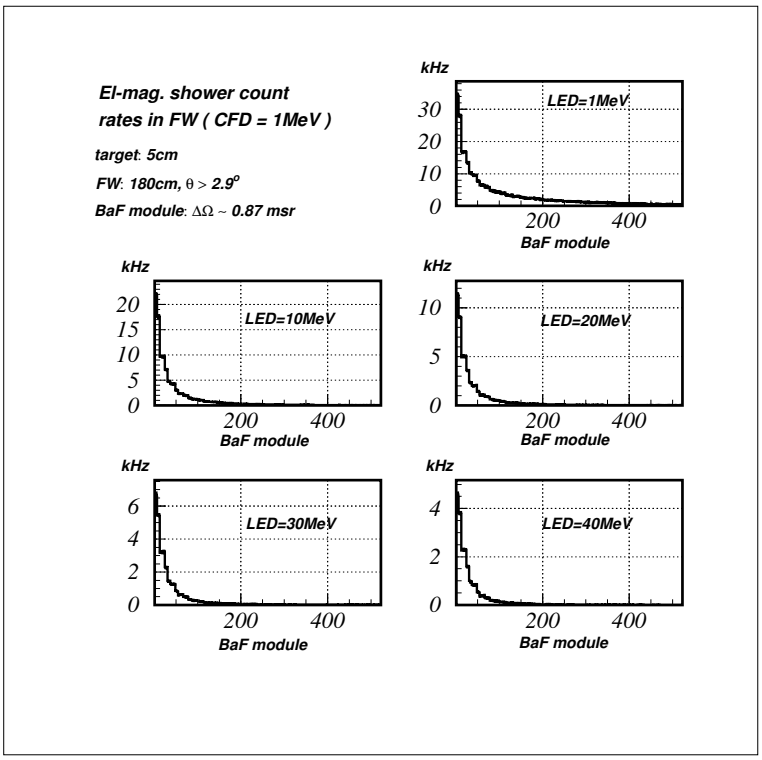

Figure 23: The rate for the beam related accidental backgrounds calculated for each individual BaF crystal. The Monte Carlo results are shown for a 5 cm long liquid hydrogen target for five different thresholds. The distance between the target and the TAPS forward wall is 180 cm.

an iterative method for each crystal. The experimentally obtained invariant mass resolutions are for π° mesons FWHM 19 MeV and for the η meson ($\eta \to 2\gamma$) FWHM 45 MeV. Altogether, the detector constitutes an ideal detection system for the observation of multi-photon events as well as protons or charged pions. Further specifications of the TAPS detector are listed in Tab. 1.

The anticipated rate for the beam related accidental backgrounds was calculated for each BaF crystal, see Fig. 23. The Monte Carlo results are shown for a 5 cm long liquid hydrogen target for five different thresholds. The distance between the target and the TAPS forward wall is 180 cm.

References

[1] R. Novotny, IEEE Trans. Nucl. Sci. 38 (1991) 379-385

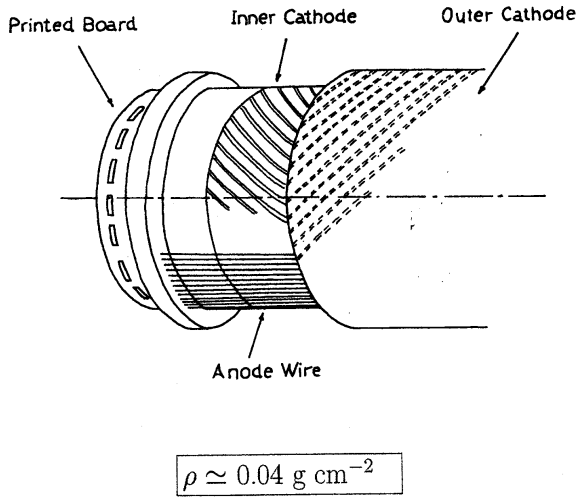

Figure 24: DAPHNE coaxial cylindrical multiware proportional chambers [1].

[2] A. R. Gabler, NIM A 346 (1994) 168-176

[3] M. Kotulla, Dipl. Thesis (1997), Justus Liebig Universitaet Giessen

E The Cylindrical Wire Chamber.

A high resolution, high efficiency central tracker detector is a vital part of the proposed experimental setup. Two coaxial cylindrical multiware proportional chambers (MWPC) developed for the DAPHNE large-acceptance tracking detector [1] will be used for this purpose. The chambers cover completely the azimuthal angular range. The length of the cylinders are so arranged as to subtend a range of angles in the polar direction Θ from 21° to 159° which corresponds to 94% of 4π sr for a source at rest.

The inner and outer cylindrical wall of the MWPC is made of 1 mm Rohacel covered with 25 μm Kapton film, see Fig. 24. The interior surfaces are laminated with aluminum strips (0.1 μm thick, 4 mm wide and separated by 0.5 mm) which form the cathode. The anode surface consists of arrays of 20 μm diameter tungsten wires stretched parallel to the cylindrical axis at 2 mm intervals around the circumference. The inner chamber has a length of 360 mm, the internal diameter is 60 mm and the external diameter is 68 mm. For the outer chamber those dimensions are 560 mm, 92 mm and 100 mm, respectively. The inner and outer cathode strips are wound helically in opposite directions at an angle of $\pm$45% with respect to the anode wires. The anode to cathode gap is 4 mm and a mixture of Ar (74.5%), ethane (25%) and freon (0.5%) is used as a filling gas.

The chamber provides a track reconstruction efficiency of $\sim$ 85% for $\pi^{\pm}$, and $\sim$ 90% for protons. The resolution for the polar and the azimuthal angles which is a function of the polar angle is expected to be $\Delta\Theta$(FWHM) $\lesssim 2°$ and $\Delta\phi$(FWHM) $\lesssim 4°$.

The cylindrical chamber as well as a straw tube prototype were tested at MAMI photon beam in order to estimate a possible events rate through the central tracker device [2] [3].

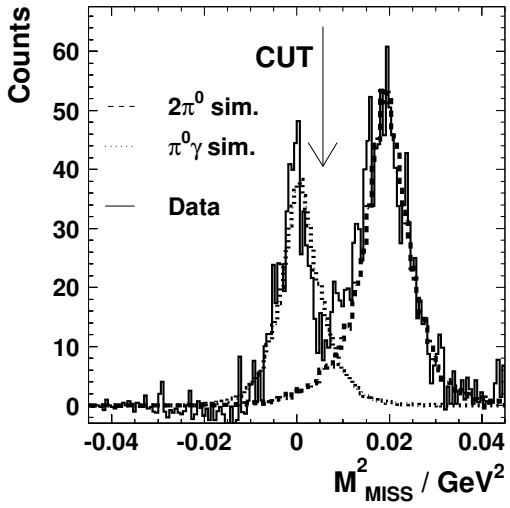

Figure 25: Missing mass of the $\pi^0 p$ final state, when an additional photon was detected. The peak near 0.02 GeV^2 originates from the $2\pi^0$ production. The peak at 0 GeV^2 is the $\gamma p \to \gamma' \pi^0 p$ reaction.

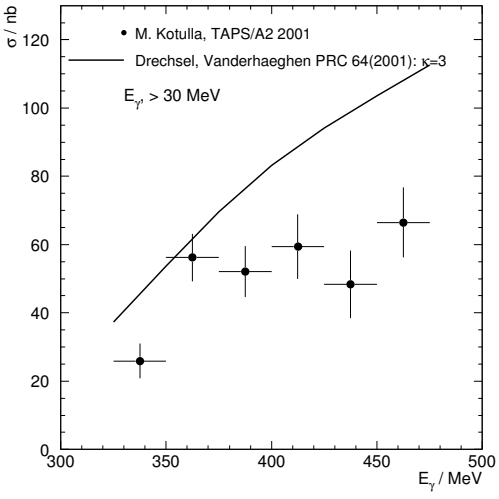

Figure 26: Total cross section for the reaction $\gamma p \to \gamma' \pi^0 p$ integrated for photon energies $E_{\gamma'} > 30 MeV$ in comparison to the calculation [7].

References

[1] G. Audi *et al*, Nucl. Instr. and Meth. **A301**, 473 (1991).

[2] A. Starostin *et al.* CB@MAMI-2-2002, internal report at http://bmkn8.physics.ucla.edu/Crystalball/Docs/documentation.html (2002).

[3] R. Beck *et al.* CB@MAMI-4-2002, internal report at http://bmkn8.physics.ucla.edu/Crystalball/Docs/documentation.html (2002).

F Targets for the Crystal Ball at MAMI

For an standard proton and deuteron target the existing horizontal cryosystem of the detector DAPHNE can be used which can liquefy ^1H, ^2H, ^3He and ^4He. The cooling system consists of two loops based on a Gifford-McMahon refrigerator which brings the ^4He coolant to 17 K, and is used to cool ^1H and ^2H targets. To obtain lower temperatures for ^3He and ^4He targets, a Joule-Thomson valve is coupled to the high pressure of the Gifford-McMahon refrigerator and a temperature of 2.5 K is reached by pumping the ^4He bath after the Joule-Thomson valve.

G TAPS $\gamma p \to \gamma' \pi^0 p$ Results

The first measurement of the reaction $\gamma p \to \gamma' \pi^0 p$ with the attempt to extract the $\Delta^+(1232)$ magnetic moment has been done by the TAPS and A2 collaborations [1, 2].

The reaction $\gamma p \to \gamma' \pi^0 p$ was measured at the electron accelerator Mainz Microtron (MAMI) [3, 4] using the Glasgow tagged photon facility [5] and the photon spectrometer

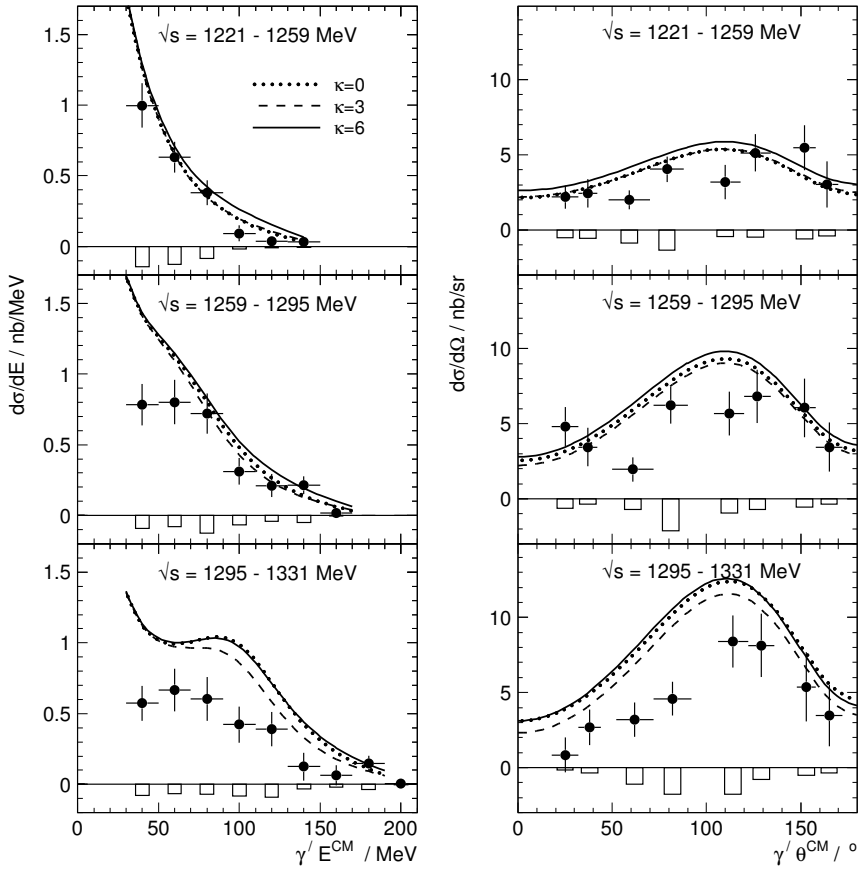

Figure 27: *Left:* Energy differential cross section for the photon γ'; on the *right* hand side the angular differential cross section in the CMS. The lines show the Drechsel, Vanderhaeghen calculation [7] for three different anomalous magnetic moments κ_{Δ^+}.

TAPS [6]. The TAPS detector consisted of six blocks each with 62 hexagonally shaped BaF_2 crystals arranged in an 8×8 matrix and a forward wall with 138 BaF_2 crystals arranged in a 11×14 rectangle. The six blocks were located in a horizontal plane around the target at angles of ±54°, ±103° and ±153° with respect to the beam axis. Their distance to the target was 55 cm and the distance of the forward wall was 60 cm. This setup covered ≈38% of the full solid angle. All BaF_2 modules were equipped with 5 mm thick plastic detectors for the identification of charged particles. The liquid hydrogen target was 10 cm long with a diameter of 3 cm. The reaction channel was exclusively measured, i.e. the fourmomenta of all particles in the final state were determined. The π° mesons were detected via their two photon decay channel and identified in a standard invariant mass analysis using the measured photon energies and momenta as input. A missing mass cut was used to seperate the $\pi^0\gamma'$ from the $2\pi^0$ background channel. Fig. 25 shows this missing mass distribution and the clean identification of the $\pi^0\gamma'$ production. The data agrees with the simulated lineshape of a GEANT Monte Carlo for both reaction channels. An additional energy balance of the particles in the initial and final state confirmed the identification.

The energy and angular differential cross section of the production photon γ' is shown in Fig. 27 in the CMS. Fig. 26 shows the total cross section for the reaction $\gamma p \to \gamma'\pi^0 p$ integrated for photon energies $E_{\gamma'} > 30$ MeV; it is roughly 60 nb. The measured number of events with the TAPS setup in 1999 is about 500 for the beam energy range of 325–475 MeV. This limited statistic certainly calls for an improved sequencing experiment using a 4π detector with high luminosity photon beam in order to measure the $\pi^0\gamma' p$ channel with high precision. The second requirement is a reliable and accurate theoretical description of the reaction $\gamma p \to \gamma'\pi^0 p$ in order to extract a precise value for the Δ^+ magnetic moment with small model dependence.

References

[1] M. Kotulla for TAPS/A2, in proceedings of the N* Conference 2001, 339-345

[2] M. Kotulla, Phd Thesis (2001), Justus Liebig Universitaet Giessen

[3] Th. Walcher et al, Prog. Part. Nucl. Phys. 24 (1990) 189-203

[4] J. Ahrens et al, Nuclear Physics News 4 (1994) 5-15

[5] I. Anthony et al, NIM A 301 (1991) 230-240

[6] R. Novotny, IEEE Trans. Nucl. Sci. 38 (1991) 379-385

[7] D. Drechsel and M. Vanderhaeghen, PRC 64 (2001) 065202

H The Crystal Ball $\pi^- p \to \pi^0\gamma n$ Preliminary Results.

The Crystal Ball 1998 AGS data at π^- beam momentum of 547 MeV/c were analyzed in a search for the $\pi^0\gamma n$ final state. The events with three photon clusters as well as with three photon and one neutron clusters were used. All three- and four-cluster events have been tested for the $\pi^- p \to \pi^0\gamma n \to 3\gamma n$ hypothesis. The kinematical fitting routine was used to

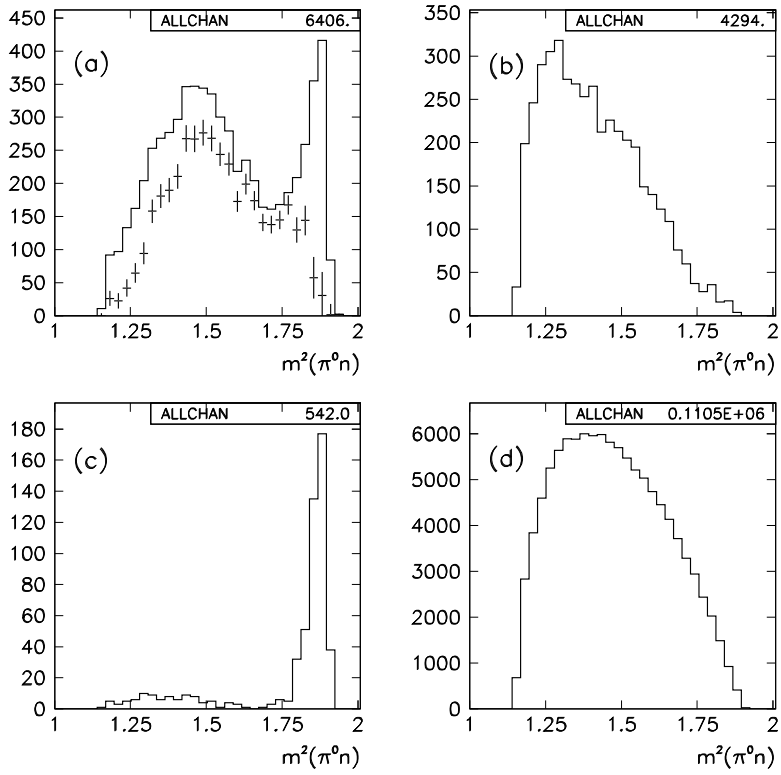

Figure 28: The disctribution of the invariant mass squared $m^2(\pi^0 n)$ for $\pi^- p \to \pi^0 \gamma n$ event candidates at $p_{\pi^-} = 547$ MeV/c. The CB data (a) are compared to the results of the Monte Carlo for $\pi^0\pi^0 n$ (b) and $\pi^0 n$ (c) background reactions. Figure (d) shows the phase-space distribution for the $\pi^0\gamma n$. The data after the background subtraction are shown in Fig. 28a by the dashed line.

calculate the χ^2. The event was accepted if it satisfied the hypothesis with a probability greater then 15%. The main background originates from the reactions

$$\pi^- p \to \pi^0 n, \tag{9}$$

$$\pi^- p \to \pi^0\pi^0 n. \tag{10}$$

The background reactions contribution was calculated with the Crystal Ball Monte Carlo. The Monte Carlo for the reactions 9 and 10 was generated according to the data measured in the same experiment. The complex dynamics of reaction 10 was reproduced by the $\pi^- p \to \Delta^0(1232)\pi^0 \to \pi^0\pi^0 n$ chain with a specific angular distribution of the $\Delta^0(1232)$ decay.

The energy spectrum for the production photon is shown in Fig 28 for the CB data compared to the results of the Monte Carlo for reactions 9 and 10. The Monte Carlo data normalized to the number of good single π^0 and $2\pi^0$ events detected were subtracted from the data. The result of the subtraction is also shown in Fig. 28a.

References

[1] S. Prakhov, CB internal report at http://bmkn8.physics.ucla.edu/Crystalball/ (2002).